Heat Diffusion Over Weighted Manifolds: A New Descriptor for Textured 3D Non-Rigid Shapes

Mostafa Abdelrahman[1,2], Aly Farag[2], David Swanson[3], and Moumen T. El-Melegy[1]
[1] Electrical Engineering Department, Assiut University, Assiut 71516, Egypt
[2] CVIP Lab, University of Louisville, Louisville, KY 40292, USA
[3] Department of Mathematics, University of Louisville, Louisville, KY 40292, USA
mostafa.abdelrahman@aun.edu.eg, {aly.farag, david.swanson}@louisville.edu, moumen@aun.edu.eg

Abstract

This paper proposes an approach for modeling textured 3D non-rigid models based on Weighted Heat Kernel Signature(W-HKS). As a first contribution, we show how to include photometric information as a weight over the shape manifold, we also propose a novel formulation for heat diffusion over weighted manifolds. As a second contribution we present a new discretization method for the proposed equation using finite element approximation. Finally, the weighted heat kernel signature is used as a shape descriptor. The proposed descriptor encodes both the photometric, and geometric information based on the solution of one equation. We also propose a new method to introduce the scale invariance for the weighted heat kernel signature. The performance is tested on two benchmark datasets. The results have indeed confirmed the high performance of the proposed approach on the textured shape retrieval problem, and showed that the proposed method is useful in coping with different challenges of shape analysis where pure geometric and pure photometric methods fail.

1. Introduction

The emergence of 3D scanners, multi-view stereo techniques and more recently consumer depth cameras have made the acquisition of 3D models easier than before. This led to a dramatic increase in the amount of 3D data available. As such the need to develop a 3D search engines has become more important. And accordingly, developing a shape search and retrieval algorithms attracted a lot of research to be able to organize and retrieve the 3D content, by using 3D descriptors and similarity measures. Several techniques and algorithms have been developed over the years for that goal. One of the key aspects of these techniques is constructing an efficient shape descriptor which is by no means a trivial task.

Recently, many sensors are able to acquire the color information besides the 3D shape, also multiple-view stereo techniques are able to recover both geometric and photometric information. These photometric features can play an important role in many shape analysis applications, such as shape matching and correspondence because it contains rich information about the visual appearance of real objects. This new requirement and its important applications adds another, new dimension to the problem difficulty. Most descriptors proposed so far are confined to shape, that is, they analyze only geometric and/or topological properties of 3D models. Therefore more efforts need to be done to consider color in addition to shape in object representation and description. The domain of research in this paper is the representation of textured shapes in order to develop an efficient descriptor that combines the color information as well as the geometric shape information. The sought representation should cope with non-rigid transformations, which is a key requirement for many target applications.

Some trials has been done to use the photometric information by the fusion of geometric and photometric information in a shape descriptors. Evaluation of 3D shape retrieval methods with respect to other several requirements can be found in [28].

1.1. Review of Related Work

There has been an extensive work on constructing descriptors for 3D shapes (e.g., [9, 26, 17, 11, 17, 16, 29, 2]). One of the challenging issues in that regard is how to handle non-rigid transformation. The problem of non-rigid shape deformation needs more work to compensate for the degrees of freedom resulting from local deformations. In the past decade, significant effort has been invested in extending the invariance properties to non-rigid deformations. Elad and Kimmel [10] proposed modeling shapes as metric spaces with the geodesic distances as an intrinsic metric, which are invariant to inelastic deformations. Bronstein

et al. [5] used this framework with a metric defined by internal distances in 2D shapes. Reuter et al. [23] used the Laplacian spectra as intrinsic shape descriptors, and they employed the Laplace-Beltrami spectra as 'shape-DNA' or a numerical fingerprint of any 2D or 3D manifold (surface or solid). They proved that 'shape-DNA' is an isometry-invariant shape descriptor. Rustamov [25] used an isometry-invariant shape representations in the Euclidean space, and then histograms of Euclidean distances to compare between shapes.

Another type of intrinsic geometry is generated by heat diffusion processes on the shape. Coifman and Lafon [20] popularized the notation of diffusion geometry, which is closely related to scale-space methods in image processing. Sun et al. [27], and [12] proposed heat kernel signatures (HKS) as deformation-invariant descriptors based on diffusion of multi-scale heat kernels. HKS is a point based signature satisfying many of the good descriptor properties but suffers from sensitivity to scale. The authors did not demonstrate how to retrieve shapes using HKS, although they pointed out the future potentials in shape retrieval applications. Bronstein et al. [7, 6] and [1] solved the HKS scale problem through a series of transformations.

All these efforts have focused only on the 3D shape. Recently, taking the photometric information into account to calculate a 3D shape descriptor has attracted more research. Liu et al. [21] proposed a method that picks points in regions of either geometry-high variation or color-high variation, and defines a signature at these points. A geometric SIFT-like descriptor for textured shapes are defined directly on the surface in [30]. The work of Kovnatsky et al. [18, 19] uses the diffusion geometry framework for the fusion of geometric and photometric information in local and global shape descriptors. Their construction is based on an *ad hoc* definition of a diffusion process on the shape manifold embedded into a high-dimensional space where the embedding coordinates represent the photometric information. Their method fails to provide a mathematical justification for their proposed heat kernel framework or the proposed discretization method. Iglesias and Kimmel [15] used the diffusion distances based on Schrodinger operators incorporating texture data, then compared the histograms of Schrodinger diffusion distances with the earth mover's distance. Finally, S. Biasotti et al. [4] proposed the PHOG descriptor as a combination of photometric, hybrid and geometric descriptions into one descriptor for textured 3D object retrieval.

1.2. Paper Contribution

In this paper, we develop, for the first time, a mathematical framework for the diffusion geometry on textured shapes. We present an approach for shape matching and retrieval based on weighted heat kernel signature. As a first contribution, we show how to include photometric information as a weight over the shape manifold. We also propose a novel formulation for heat diffusion over weighted manifolds. As a second contribution we present a new discretization method for the weighted heat kernel induced by the linear FEM weights. We also propose a new method to introduce the scale invariance for the weighted heat kernel signature. Finally, the weighted heat kernel signature is used as a shape descriptor. This proposed scale normalization method eliminates the scale effect with less sensitivity to noise. The proposed descriptor encodes both the photometric, and geometric information based on the solution of one equation. The performance is tested on two benchmark datasets SHREC'13 and SHREC'14 of textured 3D models [8, 3]. Our method outperforms all best-performing state-of-the-art methods in recent competition SHREC'13 on retrieval of textured 3D models. This can be attributed to the better capability of our method to capture object shape and texture compared to other methods as well as its better scale invariance property. Fig. 1 shows the steps for the construction of the proposed descriptor.

This paper is organized as follows. Section 2 presents some fundamental concepts, such as the heat equation and the heat kernel. Then it proposes the heat kernel on weighted manifold, and derives the new discretization method for the weighted heat kernel based on FEM. Section 3 shows how to construct a new descriptor based on the new mathematical concepts. We report our experimental results in Section 4. Conclusions and future work are given in Section 5.

2. The Heat Equation and Heat Kernel

Heat is energy transferred from one system to another by thermal interaction. The heat equation is an important partial differential equation which describes the distribution of heat (or variation in temperature) in a given region over time. One way to solve this equation is to use eigenfunctions and eigenvalues of the Laplace-Beltrami operator. In this section we will describe the solution of the heat equation on a manifold, and the weighted heat equation on a weighted manifold based on finite element approximation; also, we will give the definition of the heat kernel, and the weighted heat kernel.

Modeling the flow of heat at time t on a manifold $\mathcal{M}$, the heat equation is a second order parabolic partial differential equation [24], and is usually written as

$$\triangle_{\mathcal{M}} U(\mathbf{x}, t) = -\frac{1}{2}\frac{\partial}{\partial t} U(\mathbf{x}, t), \tag{1}$$

where $\triangle_{\mathcal{M}}$ denotes the positive semi-definite Laplace-Beltrami operator of $\mathcal{M}$, which is Riemannian equivalent of the Laplacian (Note, there can be a "conductivity"

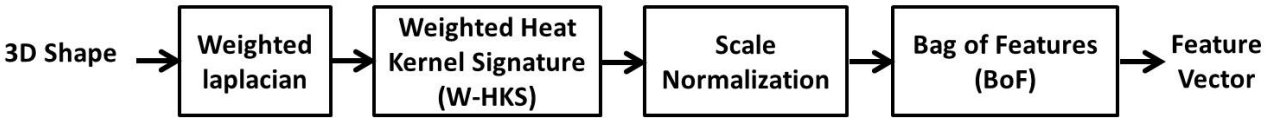

Figure 1. Construction of the proposed descriptor.

constant in the RHS that we do not use here). The solution $U(\mathbf{x},t)$ of the heat equation with initial condition $U(\mathbf{x},0) = u(\mathbf{x})$ describes the amount of heat on the surface at point $\mathbf{x}$ in time t. $U(\mathbf{x},t)$ is required to satisfy the Dirichlet boundary condition $U(\mathbf{x},t) = 0$ for all $\mathbf{x} \in \partial\mathcal{M}$ and all t.

2.1. Heat Kernel

The heat diffusion propagation over $\mathcal{M}$ is governed by the heat equation (1). Given an initial heat distribution $u : \mathcal{M} \subseteq \mathbb{R}^d \rightarrow \mathbb{R}$, as a scalar function defined on a compact manifold $\mathcal{M}$, the scale based representation $U : \mathcal{M} \times \mathbb{R} \rightarrow \mathbb{R}$ of u with, $lim_{t\rightarrow 0} U(\mathbf{x},t) = u(\mathbf{x})$ satisfies the heat equation for all t.

The heat kernel can be thought of as the amount of heat that is transferred from $\mathbf{x}$ to $\mathbf{y}$ in time t given a unit heat source at $\mathbf{x}$. Since $\mathcal{M}$ is compact then $U(\mathbf{x},t) = \int_{\mathcal{M}} K(\mathbf{x},\mathbf{y},t)u(\mathbf{y})dy$. It can be shown that the heat kernel has the following spectral decomposition

$$K(\mathbf{x},\mathbf{y},t) = \sum_{i=1}^{\infty} e^{-\lambda_i t}\phi_i(\mathbf{x})\phi_i(\mathbf{y}), \qquad (2)$$

where λ_i and ϕ_i are the i^{th} eigenvalue and the i^{th} eigenfunction of the Laplace-Beltrami operator respectively, and $\mathbf{x}$ and $\mathbf{y}$ denote two vertices (i.e. $\triangle_{\mathcal{M}}\phi_i(\mathbf{x}) = \lambda_i\phi_i(\mathbf{x})$ for all $\mathbf{x}$.

The heat kernel $K(\mathbf{x},\mathbf{y},t)$ has many good properties [27, 14]: It is symmetric, invariant under isometric deformations, which is a direct consequence of the invariance of the Laplace-Beltrami operator. It is informative: by only considering its restriction to the temporal domain, we can obtain a concise and informative signature. It is multi-scale: for different values of t the heat kernel reflects local properties of the shape around $\mathbf{x}$ at small t and the global structure of $\mathcal{M}$ from the point of view of $\mathbf{x}$ at large values of t, and it is stable under perturbations of the underlying manifold.

This is the classical heat kernel, in the following subsection we will introduce our new formulation for the weighted heat kernel.

2.2. Heat Kernel on Weighted Manifold

A weighted manifold (called also a manifold with density) [13] is a Riemannian manifold $\mathcal{M}$ endowed with a measure μ that has a smooth positive density h with respect

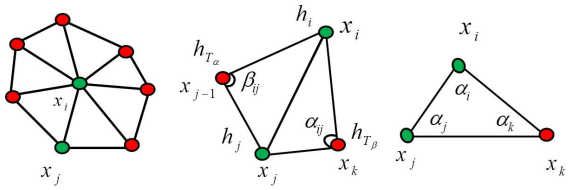

Figure 2. Discrete triangulated surface. Left:A vertex $\mathbf{x}_i$ and its adjacent faces. Middle: the definition of the angles α_{ij} and β_{ij} and the weights h_i, h_j, h_{T_α} and h_{T_β}. Right: the definition of the interior angles α_i, α_j, α_k of triangle T at vertices i, j, k respectively.

to the Riemannian measure σ. The weighted Laplace operator $\triangle_{\mathcal{M},\mu}$, generalizing the Laplace-Beltrami operator, is defined by

$$\begin{aligned} \triangle_{\mathcal{M},\mu}U &= div_\mu \nabla U \\ &= \frac{1}{h} div(h\nabla U) \\ &= \frac{1}{h\sqrt{detg}}\frac{\partial}{\partial x_i}(h\sqrt{detg})\frac{\partial}{\partial x_i}U \end{aligned} \qquad (3)$$

for any smooth function U on $\mathcal{M}$, where g be the Riemannian metric on $\mathcal{M}$. It is possible to extend $\triangle_{\mathcal{M},\mu}$ to a self-adjoint operator in $L^2(\mathcal{M},\mu)$, which allows one to define the heat semigroup $e^{-t\triangle_{\mathcal{M},\mu}}$. The heat semigroup has the integral kernel $K_t(x,y)$, called the heat kernel of $(\mathcal{M},\mu)$.

We propose the weighted heat equation

$$\triangle_{\mathcal{M},\mu}U(\mathbf{x},t) = -\frac{1}{2}\frac{\partial}{\partial t}U(\mathbf{x},t) \qquad (4)$$

with initial condition $U(\mathbf{x},0) = u(\mathbf{x})$ and Dirichlet boundary condition $U(\mathbf{x},t) = 0$ for all $\mathbf{x} \in \partial\mathcal{M}$ and all $t > 0$.

2.3. Finite Element Discretization of the Weighted Heat Equation

The weak formulation of the weighted heat equation (4) is obtained by multiplying by a test function $\varphi \in \mathcal{C}^2$ and integrating the resulting relation over the weighted manifold $(\mathcal{M},\mu)$

$$\int_{\mathcal{M}} \varphi\frac{\partial}{\partial t}U(\mathbf{x},t)d\mu + \frac{1}{2}\int_{\mathcal{M}} \varphi\triangle_{\mathcal{M},\mu}U(\mathbf{x},t)d\mu = 0 \qquad (5)$$

where $d\mu = hd\sigma$, $d\sigma$ is the Riemannian measure and h is a smooth positive density. Then, by writing the weighted

Laplacian in terms of the divergence we get

$$\int_{\mathcal{M}} \varphi \frac{\partial}{\partial t} U h d\sigma + \frac{1}{2} \int_{\mathcal{M}} div(h \nabla U) \varphi d\sigma = 0, \quad (6)$$

Using the Green formula we get,

$$\int_{\mathcal{M}} \varphi \frac{\partial}{\partial t} U h d\sigma + \frac{1}{2} \int_{\mathcal{M}} (h \nabla U).\nabla \varphi d\sigma = 0. \quad (7)$$

We thus obtain the weak formulation of (4)

$$\int_{\mathcal{M}} \varphi \frac{\partial}{\partial t} U d\mu + \frac{1}{2} \int_{\mathcal{M}} (\nabla U.\nabla \varphi) d\mu = 0 \quad (8)$$

Let $\mathcal{B} = \{\varphi_i\}_{i=1}^n$ be a family of n linearly independent C^2 functions. We form an approximation $\tilde{U}(\mathbf{x}, t)$ to $U(\mathbf{x}, t)$ by

$$\tilde{U}(\cdot, t) := \sum_{i=1}^{n} a_i(t) \varphi_i, \quad t > 0. \quad (9)$$

Replacing U by $\tilde{U}$ in (8) we obtain

$$\sum_{i=1}^{n} B(i,j) \frac{\partial}{\partial t} a_i(t) + \frac{1}{2} \sum_{i=1}^{n} L(i,j) a_i(t) = 0 \quad (10)$$

where

$$B(i,j) = \int_{\mathcal{M}} \varphi_i \varphi_j h d\sigma, \quad (11)$$

and

$$L(i,j) = \int_{\mathcal{M}} (\nabla \varphi_i . \nabla \varphi_j) h d\sigma. \quad (12)$$

To discretize (10) we let $\mathcal{N} = (M; T)$ be a triangulated surface that approximates $\mathcal{M}$. Here $M := \{\mathbf{x}_i; i = 1, \ldots, n\}$ is a set of n vertices and T is an abstract simplicial complex containing the adjacency information. We choose linearly independent basis functions $\mathcal{B} = \{\varphi_i\}_{i=1}^n$, where $\varphi_i(\mathbf{x}_j) = \delta_{ij}$ is equal to 1 at vertex i, 0 at all other vertices, and linearly interpolates between 1 and 0 on all triangles incident to vertex i. Label vertex $\mathbf{x}_i$ simply as i. If i, j, k are the distinct vertices of a triangle T, then $\alpha_i, \alpha_j, \alpha_k$ denote the interior angles of T at vertices i, j, k respectively, and $A(T)$ is the area of T as shown in Fig. 2, and since h is piecewise linear we can substitute h in Eq. 11 and Eq. 12 by $h_i \varphi_i + h_j \varphi_j + h_k \varphi_k$. Then it can be shown that:

$$\begin{aligned}
\nabla \varphi_i . \nabla \varphi_j &= -\frac{\cot \alpha_k}{2A(T)} \\
| \nabla \varphi |^2 &= \frac{\cot \alpha_j + \cot \alpha_k}{2A(T)} \\
\int_T \varphi_i d\sigma &= \frac{A(T)}{3} \\
\int_T \varphi_i^2 d\sigma &= \frac{A(T)}{6} \\
\int_T \varphi_i \varphi_j d\sigma &= \frac{A(T)}{12} \\
\int_T \varphi_i^3 d\sigma &= \frac{A(T)}{10} \\
\int_T \varphi_i^2 \varphi_j d\sigma &= \frac{A(T)}{30} \\
\int_T \varphi_i \varphi_j \varphi_k d\sigma &= \frac{A(T)}{60}
\end{aligned}$$

Denote by h_{T_k} the average value of a function h over a triangle T_k. Denote by $N_e(i)$ the set of vertices adjacent to i. Given $j \in N_e(i)$ denote by T_α and T_β the triangles having (i, j) as an edge and by α and β the interior angles of T_α and T_β opposite edge (i, j). Then

$$B(i,j) = \begin{cases} (h_i + h_j) \frac{A(T_\alpha) + A(T_\beta)}{60} + \\ \quad \frac{h_{T_\alpha} A(T_\alpha) + h_{T_\beta} A(T_\beta)}{20} & if\ j \in N_e(i) \\ \sum_{k \in N_e(i)} A(T_k) (\frac{h_i}{15} + \frac{h_{T_k}}{10}) & if\ i = j \end{cases} \quad (13)$$

where T_k is the counter-clockwise oriented triangle with vertices i and k, and $B(i, j) = 0$ whenever i and j are nonadjacent vertices. Likewise, $L(i, j)$ is given by

$$L(i,j) = \begin{cases} -\frac{h_{T_\alpha} \cot \alpha + h_{T_\beta} \cot \beta}{2} & if\ j \in N_e(i) \\ \sum_{k \in N_e(i)} L(i,k) & if\ i = j \end{cases} \quad (14)$$

and $L(i, j) = 0$ otherwise.

To compute the solution to 4, let us consider the generalized eigensystem $\{\lambda_i, \phi_i\}_{i=1}^n$ of (L, B), which satisfies the relations $L\phi_i = \lambda_i B \phi_i, i = 1, \ldots, n$. Since the Laplacian eigenvectors $\{\phi_i\}_{i=1}^n$ form a basis of $\mathbb{R}^n$ and $(\tilde{U}(\mathbf{x}, t))_{i=1}^n \in \mathbb{R}^n$, for any $t \in \mathbb{R}^+$ we express the solution $\tilde{U}(\cdot, t) := \sum_{i=1}^n a_i(t) \phi_i$ where $\mathbf{a} = (a_i(t))_{i=1}^n$ is the unknown vector.

After solving for the coefficients $a_i(t)$, then $a_i(t) = exp(-\frac{1}{2}\lambda_i t) \langle u(\mathbf{x}), \phi_i \rangle_B$ where $u(\mathbf{x})$ is the initial value of $\tilde{U}(\mathbf{x}, t)$. Then,

$$\tilde{U}(\cdot, t) := \sum_{i=1}^{n} exp(-\frac{1}{2}\lambda_i t) \langle u(\mathbf{x}), \phi_i \rangle_B \phi_i, \quad (15)$$

or in a matrix form

$$\tilde{U}(\cdot,t) := \phi D(t)\phi^T B u(\mathbf{x}) \tag{16}$$

where $\phi = [\phi_1, \phi_2, \ldots, \phi_n]$, and
$D(t) = diag(exp(-\frac{1}{2}\lambda_1 t), exp(-\frac{1}{2}\lambda_2 t), \ldots, exp(-\frac{1}{2}\lambda_n t))$.

Then the heat kernel will be

$$K(\mathbf{x},\mathbf{y},t) := \phi D(t)\phi^T B, \tag{17}$$

and the weighted heat kernel signature will be

$$K(\mathbf{x},\mathbf{x},t) := B\phi^2 diag(D(t)) \tag{18}$$

The heat kernel signature was introduced by [27, 7, 6] as an intrinsic local shape descriptor based on diffusion scale-space analysis. Here we introduce the weighted version by considering the color information at each vertex as the weight h as discussed earlier.

3. Proposed Descriptor

In this section, we propose an approach for shape modeling and retrieval using weighted heat kernel signature. Fig. 1 shows the steps for the construction of the proposed descriptor. The proposed descriptor is based on the BoF representation of the W-HKS calculated all shape vertices at different time scales. We propose a novel method to achieve scale-invariance of HK which is shown to be noise-robust. The scale normalization step is applied to the W-HKS before the BoF representation as explained in the following subsection. The proposed descriptor is compact in size, and efficient in computation.

3.1. Scale Invariance

Scale invariance is a desirable property of the shape descriptor, which can be achieved by different methods: by trying to detect the scale, as done in most feature descriptors (e.g. SIFT) in image analysis, through the normalization of Laplace-Beltrami eigenvalues, using a series of transformations applied to the HKS [7] in order to avoid scale detection, or by using local equi-affine invariant Laplace-Beltrami operator proposed by [22].

In this work, we propose a local scale normalization method based on simple operations. It was shown [7] that scaling a shape by a factor β results in changing $K(x,t)$ to $\beta^2\ K(x,\beta^2 t)$. Thus, a series of transformations are applied to W-HKS as follows. Starting from each point x, the W-HKS is sampled logarithmically in time ($t = \alpha^\tau$) and the function

$$k_\tau = K(x,\alpha^\tau) \tag{19}$$

is formed. Scaling the shape by β results in a time shift $s = 2\log_\alpha \beta$ and amplitude scaling by β^2. That is,

$$k'_\tau = \beta^2 k_{\tau+s} \tag{20}$$

We propose to apply the Fourier transform directly to k'_τ in (20), similar method used in [1].

$$K'(w) = \beta^2 K(w)\exp(j\ 2\pi\ w\ s). \tag{21}$$

Then taking the amplitude of the FT,

$$\mid K'(w) \mid = \beta^2 \mid K(w) \mid \tag{22}$$

The effect of the multiplicative constant β^2 is eliminated by normalizing the $\mid K'(w) \mid$ by the sum of the amplitudes of the FT components. The amplitudes of the first significant FT components (we normally use 20) are employed to construct the scale-invariant shape descriptor. This proposed method eliminates the scale effect without having to use the noise-sensitive derivative operation or the logarithmic transformation that both were used in [7]. An experiment comparing the two methods against noise, with considerably superior performance for our method.

3.2. Shape/Color Descriptor

We propose to construct the descriptor as follows: The W-HKS descriptor is calculated for each triangle mesh based on Eq. 18. We calculated the W-HKS at all points of a shape over the three normalized color channels (RGB). The color information is considered as the weight h at each vertex as shown in Fig. 2 middle: the definition of the weights $h_i, h_j, h_{T_\alpha},\ and\ h_{T_\beta}$. W-HKS is calculated at different time scales, we used a logarithmic scale-space with base $\alpha = 2$ and τ ranging form 0.01 to 8 with step $1/16$ for each color band. Investigating other possible color spaces has been done, using RGB have approved better performance than other color spaces, and using three bands have approved better performance that grayscale. Then the scale normalization step is applied as explained in Sec. 3.1. Considering only the first 20 significant FT components the size of the descriptor now will be $n \times 20$ for n vertex shape. Then we used the Bag of Features (BoF) to represent the shape as one feature vector. The bags of features were created using the same vocabulary of size 64. Thus the feature vector size is 64×3 for any 3D shape.

4. Experimental Results

To test the performance of the proposed approach we use the SHREC'13 dataset [8] and the SHREC'14 dataset [3]. SHREC'13 dataset is a collection made of 240 texture shapes, organized in 10 classes, each with 24 models. Each class (humans, four legs animals, vases etc.) contains six null models, that is, two base meshes endowed with three different textures. Each null shape is then modified via four transformations, including two non-metric-preserving deformations, one non-rigid deformation, and one additive Gaussian noise perturbation. All transformations are applied at different strength levels for the ten classes. Also, the

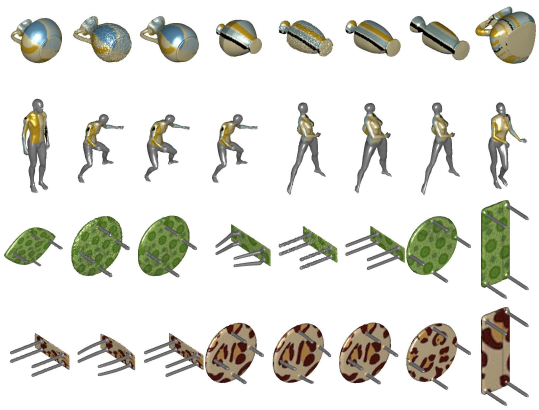

Figure 3. Sample of 4 different classes of the SHREC'13 benchmark [8] with different texture and deformation show the challenge of the dataset. For each null shape there are a transformed versions of it that include non-rigid deformation, nonmetric-preserving deformations, and additive Gaussian noise perturbation.

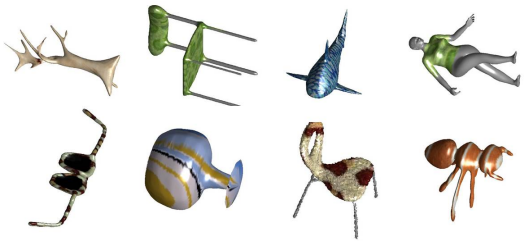

Figure 4. Sample of 8 different classes of the SHREC'14 benchmark [3].

same texture may be shared by models in different classes, see Fig. 3.

SHREC'14 dataset is made of 572 watertight mesh models, grouped in thirteen texture and sixteen geometric classes. Each class contains twelve null models, corresponding to four base meshes endowed with three different textures. Then, three transformations are applied to each null shape. The three transformations randomly combine a geometric deformation (re-sampling, addition of Gaussian noise, an affine deformation, and two non-isometric deformations) with a texture one (lightening/darkening, topological deformations in the texture patterns, affine transformations in the RGB channels). Samples of the geometric classes in the dataset are given in Fig. 4.

We compare our method with the four best methods in the retrieval competition on textured 3D models [8]: a method based on Scale Invariant Heat Kernels combined with the color histogram(A2), the Color-weighted Histograms of Area Projection Transform (G1), a method based on 2D multi-view and bag-of-features approach (G2), and one method merging a shape description based on geodesic distance matrices with RGB histograms (V2) [8]. We also

Run	NN	1-Tier	2-Tier	ADR
A2	0.508	**0.561**	**0.730**	0.380
W-HKS1	**0.7765**	0.5350	0.6458	**0.4047**

Table 1. Results on SHREC'13 dataset compares the proposed descriptor (W-HKS1) against the (A2) based on Scale Invariant Heat Kernels combined with the color histogram.

compare our results against the PHOG approach proposed in [4].

We use the average precision-recall curves, Nearest Neighbor (NN), First Tier (FT), Second Tier (ST), and Average Dynamic Recall (ADR) [26] as evaluation measures. To compute these measures, we assume two objects belong to the same class if they share both geometric and texture information. The final score is the average on all possible queries and it is always less than 1.

Table 1 lists the average measures over all classes in the SHREC'13 dataset, and Table 2 lists the average measures over all classes in the SHREC'14 dataset. The table compares the proposed descriptor (W-HKS1) against the (A2) based on Scale Invariant Heat Kernels combined with the color histogram. The NN and ADR measures prove that the proposed descriptor has better performance because it encodes the color as well as the geometric information.

Another version, called (W-HKS2), of the proposed descriptor is formed by appending the color histogram to the original descriptor (W-HKS1). Table 3, lists the average measures on the SHREC'13 dataset. The table compares the proposed descriptor (W-HKS2) against the five different methods. The highest measures (in bold) clearly show that the proposed descriptor has the best performance.

Fig. 5 shows some retrieval results in the SHREC'13 dataset [8], and Fig. 6 shows some retrieval results in the SHREC'14 dataset [3]. The models are ordered from left to right. The first column represents the query model. The retrieved objects per each query are ranked from left to right based on the distance measure (L1-Norm) between the query and all shapes in the dataset. We show only the first 15 retrieved models. These figures clearly demonstrate the high retrieval rate of the approach. It can be observed that the proposed method has retrieved the similar shapes with similar texture first.

Fig. 7 shows the performances of all methods in terms of average precision-recall curves in the SHREC'13 dataset [8]. The larger the area below such a curve, the better the performance under examination. This figure shows that the proposed descriptor indeed achieves the highest performance over the other five methods.

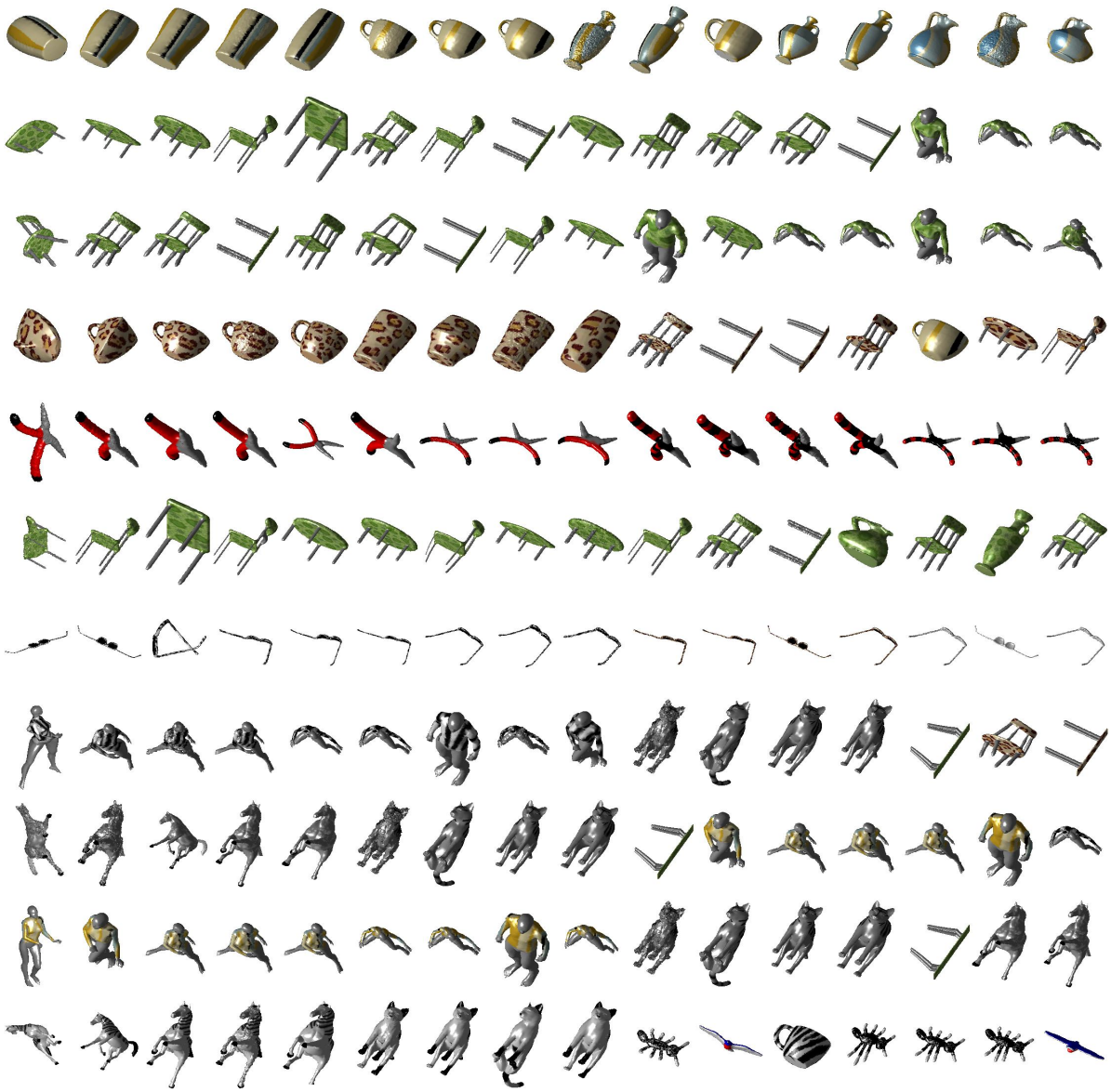

Figure 5. Shape retrieval results of SHREC'13 dataset. Left: queries. Right: First 15 matches using the W-HKS2 descriptor.

	Relevant			Highly Relevant			
Run	NN	1-Tier	2-Tier	NN	1-Tier	2-Tier	ADR
HKS + Color Hist	0.735	**0.408**	**0.521**	0.123	0.228	0.351	0.206
W-HKS1	**0.817**	0.296	0.396	**0.443**	**0.248**	**0.336**	**0.236**

Table 2. Results on SHREC'14 dataset compares the proposed descriptor (W-HKS1) against the (A2) based on Scale Invariant Heat Kernels combined with the color histogram.

5. Conclusions

This paper has addressed the problem of textured 3D shapes representation. We have presented a new approach for shape matching and retrieval based on Weighted Heat Kernel Signature (W-HKS). We proposed to use the color information as a weight over the shape manifold. We also proposed a novel formulation for heat diffusion over weighted manifolds. Then we presented a new discretization method for the weighted heat kernel based on FEM. We also proposed a new method to introduce the scale in-

Figure 6. Shape retrieval results of SHREC'14 dataset. Left: queries. Right: First 15 matches using the W-HKS2 descriptor.

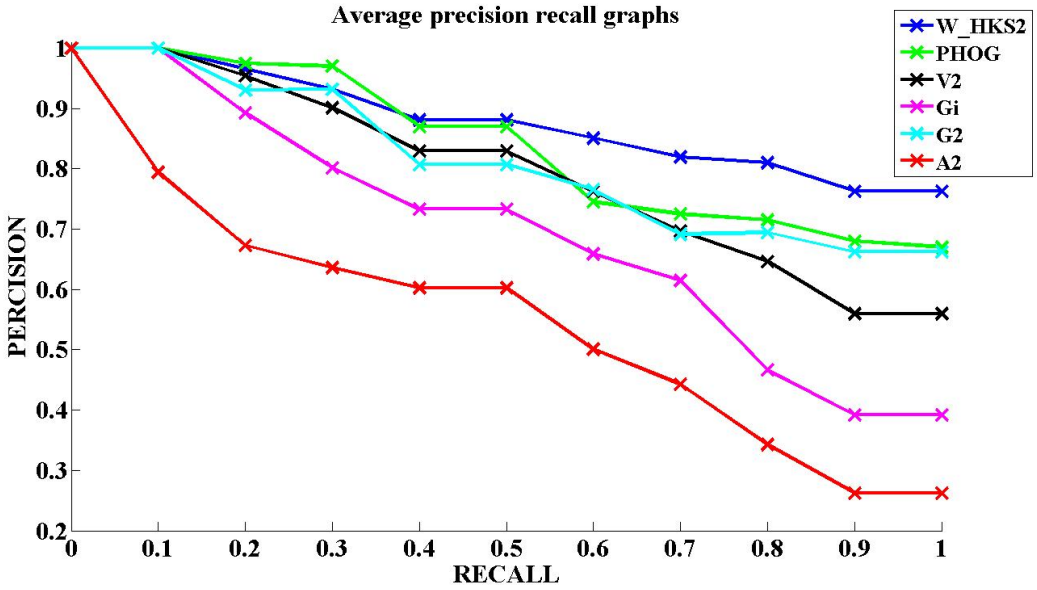

Figure 7. Shape retrieval results of SHREC'13 dataset. Precision-recall curves for all methods.

Run	NN	1-Tier	2-Tier	ADR
A2	0.508	0.561	0.730	0.380
G1	0.788	0.658	0.748	0.470
G2	0.898	0.733	0.893	0.508
V2	0.879	0.764	0.904	0.520
PHOG	**0.951**	0.773	0.899	0.534
W-HKS2	0.9242	**0.8338**	**0.9257**	**0.5701**

Table 3. Results on SHREC'13 dataset lists the average measures on SHREC'13 dataset. The table compares the proposed descriptor (W-HKS2) against five different methods.

variance for the weighted heat kernel signature. The "bag of features" (BoF) approach is used to construct compact and informative shape descriptors. Finally, the weighted heat kernel signature is used as a shape descriptor. Our experimental results have shown that the proposed descriptor can achieve high performance on SHREC'13 and SHREC'14 benchmark datasets. The proposed approach has outperformed state-of-the-art approaches (five different methods) for textured shapes representation and retrieval. Different evaluation measures approved the high accuracy of the proposed framework.

References

[1] M. Abdelrahman, M. T. El-Melegy, and A. A. Farag. 3d object classification using scale invariant heat kernels with collaborative classification. In *NORDIA ECCV Workshops*, pages 22–31, 2012.

[2] M. Ben-Chen and C. Gotsman. Characterizing shape using conformal factors. In *3DOR*, pages 1–8, 2008.

[3] S. Biasotti, A. Cerri, M. Abdelrahman, M. Aono, A. B. Hamza, M. T. El-Melegy, A. A. Farag, V. Garro, A. Giachetti, D. Giorgi, A. Godil, C. Li, Y. Liu, H. Y. Martono, C. Sanada, A. Tatsuma, S. Velasco-Forero, and C. Xu. Shrec'14 track: Retrieval and classification on textured 3d models. In *Eurographics Workshop on 3D Object Retrieval, Strasbourg, France, 2014. Proceedings*, pages 111–120, 2014.

[4] S. Biasotti, A. Cerri, D. Giorgi, and M. Spagnuolo. Phog: Photometric and geometric functions for textured shape retrieval. *Comput. Graph. Forum*, 32(5):13–22, 2013.

[5] A. M. Bronstein, M. M. Bronstein, A. M. Bruckstein, and R. Kimmel. Analysis of two-dimensional non-rigid shapes. *International Journal of Computer Vision*, 78(1):67–88, 2008.

[6] A. M. Bronstein, M. M. Bronstein, L. J. Guibas, and M. Ovsjanikov. Shape google: Geometric words and expressions for invariant shape retrieval. *ACM Trans. Graph.*, 30(1):1, 2011.

[7] M. M. Bronstein and I. Kokkinos. Scale-invariant heat kernel signatures for non-rigid shape recognition. In *CVPR*, pages 1704–1711, 2010.

[8] A. Cerri, S. Biasotti, M. Abdelrahman, J. Angulo, K. Berger, L. Chevallier, M. T. El-Melegy, A. A. Farag, F. Lefebvre, A. Giachetti, H. Guermoud, Y.-J. Liu, S. Velasco-Forero, J.-R. Vigouroux, C.-X. Xu, and J.-B. Zhang. Shrec'13 track: Retrieval on textured 3d models. In *3DOR*, pages 73–80, 2013.

[9] P. Daras and A. Axenopoulos. A 3d shape retrieval framework supporting multimodal queries. *International Journal of Computer Vision*, 89(2-3):229–247, 2010.

[10] A. Elad and R. Kimmel. Bending invariant representations for surfaces. In *CVPR (1)*, pages 168–174, 2001.

[11] M. Elad, A. Tal, and S. Ar. Content based retrieval of vrml objects - an iterative and interactive approach. pages 97–108, 2001.

[12] K. Gebal, J. A. Bærentzen, H. Aanæs, and R. Larsen. Shape analysis using the auto diffusion function. *Comput. Graph. Forum*, 28(5):1405–1413, 2009.

[13] A. Grigoryan. Heat kernels on weighted manifolds and applications. *Cont. Math. 398*, pages 93–191, 2006.

[14] E. P. Hsu. *Stochastic Analysis on Manifolds*. American Mathematical Society, 2002.

[15] J. A. Iglesias and R. Kimmel. Schrödinger diffusion for shape analysis with texture. In *ECCV Workshops (1)*, pages 123–132, 2012.

[16] A. E. Johnson and M. Hebert. Using spin images for efficient object recognition in cluttered 3d scenes. *IEEE Trans. Pattern Anal. Mach. Intell.*, 21(5):433–449, 1999.

[17] M. M. Kazhdan, T. A. Funkhouser, and S. Rusinkiewicz. Symmetry descriptors and 3d shape matching. In *Symposium on Geometry Processing*, pages 117–126, 2004.

[18] A. Kovnatsky, M. M. Bronstein, A. M. Bronstein, and R. Kimmel. Photometric heat kernel signatures. In *Scale Space and Variational Methods in Computer Vision*, pages 616–627. Springer, 2012.

[19] A. Kovnatsky, D. Raviv, M. M. Bronstein, A. M. Bronstein, and R. Kimmel. Geometric and photometric data fusion in non-rigid shape analysis. *Numerical Mathematics: Theory, Methods and Applications (NM-TMA)*, 6(1):199–222, 2013.

[20] S. Lafon, Y. Keller, and R. R. Coifman. Data fusion and multicue data matching by diffusion maps. *IEEE Trans. Pattern Anal. Mach. Intell.*, 28(11):1784–1797, 2006.

[21] Y.-J. Liu, Y.-F. Zheng, L. Lv, Y. Xuan, and X. Fu. 3d model retrieval based on color + geometry signatures. *The Visual Computer*, 28(1):75–86, 2012.

[22] D. Raviv, M. M. Bronstein, A. M. Bronstein, R. Kimmel, and N. A. Sochen. Affine-invariant diffusion geometry for the analysis of deformable 3d shapes. In *CVPR*, pages 2361–2367, 2011.

[23] M. Reuter, F.-E. Wolter, M. E. Shenton, and M. Niethammer. Laplace-beltrami eigenvalues and topological features of eigenfunctions for statistical shape analysis. *Computer-Aided Design*, 41(10):739–755, 2009.

[24] I. Rubinstein and L. Rubinstein. *Partial Differential Equations in Classical Mathematical Physics*. Cambridge University Press, 1998.

[25] R. M. Rustamov. Laplace-beltrami eigenfunctions for deformation invariant shape representation. In *Symposium on Geometry Processing*, pages 225–233, 2007.

[26] P. Shilane, P. Min, M. M. Kazhdan, and T. A. Funkhouser. The princeton shape benchmark. In *SMI*, pages 167–178, 2004.

[27] J. Sun, M. Ovsjanikov, and L. J. Guibas. A concise and provably informative multi-scale signature based on heat diffusion. *Comput. Graph. Forum*, 28(5):1383–1392, 2009.

[28] J. W. H. Tangelder and R. C. Veltkamp. A survey of content based 3d shape retrieval methods. *Multimedia Tools Appl.*, 39(3):441–471, 2008.

[29] R. Toldo, U. Castellani, and A. Fusiello. Visual vocabulary signature for 3d object retrieval and partial matching. In *3DOR*, pages 21–28, 2009.

[30] A. Zaharescu, E. Boyer, and R. Horaud. Keypoints and local descriptors of scalar functions on 2d manifolds. *International Journal of Computer Vision*, 100(1):78–98, 2012.